



# Magnetic Resonance Imaging of Iron Overload among Beta- Thalassemia Patients

Heba F. Tantawy, Esraa Abdallah, Khalid Shawky, Marwa Elsayed Abd Elhamed

Radiodiagnosis Department, Faculty of Medicine - Zagazig University, Egypt

**Article History:** Received 10<sup>th</sup> June, Accepted 5<sup>th</sup> July, published online 10<sup>th</sup> July 2023

## Abstract

**Background:** Heart failure due to iron overload is the most common cause of death in  $\beta$  thalassemia patients. Recent developments in the treatment of iron overload with improved chelation therapy have dramatically increased the expected lifespan of patients with  $\beta$ -thalassemia from less than twenty years in the 1960s to greater than forty years today. studies have shown that blood iron levels and liver iron measurements donot directly correlate with cardiac iron levels, as the hepatic and cardiactissues have different mechanisms and kinetics of iron uptake, storage and clearance. Therefore, assessing risk of heart failure from blood iron concentration or liver biopsy may not be accurate. MRI offers a noninvasive imaging study for assessment of tissue iron levels, and can be used to monitor iron burden in the heart and liver so that patients at risk for cardiac and liver failure can potentially be identified before lethal symptoms develop. MRI is increasingly being used worldwide to follow organ iron overload in  $\beta$  thalassemia patients, but can also be used to assess other types of patients with iron overload states including sickle cell disease and hemochromatosis.

**Keywords:** Magnetic Resonance Imaging, Beta-Thalassemia, Iron Overload

**DOI:** 10.53555/ecb/2023.12.Si12.280

Heart failure due to iron overload is the most common cause of death in  $\beta$  thalassemia patients. Recent developments in the treatment of iron overload with improved chelation therapy have dramatically increased the expected lifespan of patients with  $\beta$ -thalassemia from less than twenty years in the 1960s to greater than forty years today.studies have shown that blood iron levels and liver iron measurements donot directly correlate with cardiac iron levels, as the hepatic and cardiactissues have different mechanisms and kinetics of iron uptake, storage and clearance. Therefore, assessing risk of heart failure from blood iron concentration or liver biopsy may not be accurate (1)

MRI offers a noninvasive imaging study for assessment of tissue iron levels, and can be used to monitor iron burden in the heart and liver so that patients at risk for cardiac and liver failure can potentially be identified before lethal symptoms develop. MRI is increasingly being used worldwide to follow organ iron overload in  $\beta$  thalassemia patients, but can also be used to assess other types of patients with iron overload states including sickle cell disease and hemochromatosis .(2)

MRI is the most accurate and widely available non-invasive tool to assess liver iron. The main advantages of MRI include a low-rate of variability between measurements and the ability to assess iron loading in endocrine tissues, the heart and the liver (1)

MRI measures iron content in all organs, is widely available, and has been validated for measuring liver iron content. The specialized application of MRI was approved by the Food and Drug Administration for the measurement of liver iron. MRI limitations include expense, the need for trained personnel for acquisition and post-processing, and the necessity of standardizing the technique prior to its implementation .(1)

MRI operates like many imaging modalities in that it transmits a signal into the body and creates an image from the signal returning from the body after it has interacted with the microenvironment. With MRI, the transmitted signal is a microwave which excites water protons in the body to higher magnetic energy states. As these water protons relax back to the unexcited state, they emit microwaves that are received and interpreted by the scanner. In non-iron overloaded tissues, the magnetic environment is fairly magnetically homogeneous. This means that the signals received from different areas in the tissue remain coherent with one another and the signals last for a long duration (bright images without much contrast). Iron deposits high-molecular-weight iron complexes such as ferritin, haemosiderin and ferrioxamine with water molecules. Ferrioxamine is produced after cellular uptake of DFO, and in extrahepatic tissues, where there is no active excretion and it may remain for days. Ferrioxamine-based agents have been used in the past as contrast media because of their T2\* effect. However, they act like little magnets when placed in a strong magnetic field; protons diffusing along different paths experience wildly different magnetic profiles, disrupting coherence among the protons and darkening the image more quickly (3)

The MRI scanner can refocus the returning signal either using a special radiofrequency pulse (forming a so-called spin echo), or by using special small magnets known as gradients (forming a so-called gradient echo). The time constant for a spin echo is known as T2 and for a gradient echo is known as T2\*. The greater the tissue iron, the shorter the signal half lives, and the smaller the T2 and T2\* become. (4)

In fact, this darkening process behaves similarly to radioactive material and can be described by a 'half life'. The greater the tissue iron, the shorter the signal half lives, and the smaller the T2 and T2\* (measured in ms) become. This process is known as relaxation, and is characterized by the relaxation rates R2 and R2\* (measured in Hz). These rates are just the mathematical inverse of the characteristic relaxation times, T2 and T2\*. The higher the iron concentration, the higher the relaxation rates. (5)

The factor of 1000 is used because T2 and T2\* are usually reported in ms and the units of R2 and R2\* (rate of signal decay) are Hertz or s<sup>-1</sup>. So a T2\* of 20 ms is equal to an R2\* of 50 Hz and vice versa

$$R2 = 1000/T2$$

$$R2* = 1000/T2*$$

The advantage of R2 and R2\* notation is that these parameters are directly proportional to iron, rather than T2 and T2\* inversely proportional to iron; For historical reasons, results in the liver are typically reported as R2 and R2\* values whereas T2 and T2\* reporting is more common in the heart. One can also report rates of signal decay, R2 or R2\*, instead of the half-lives (1).

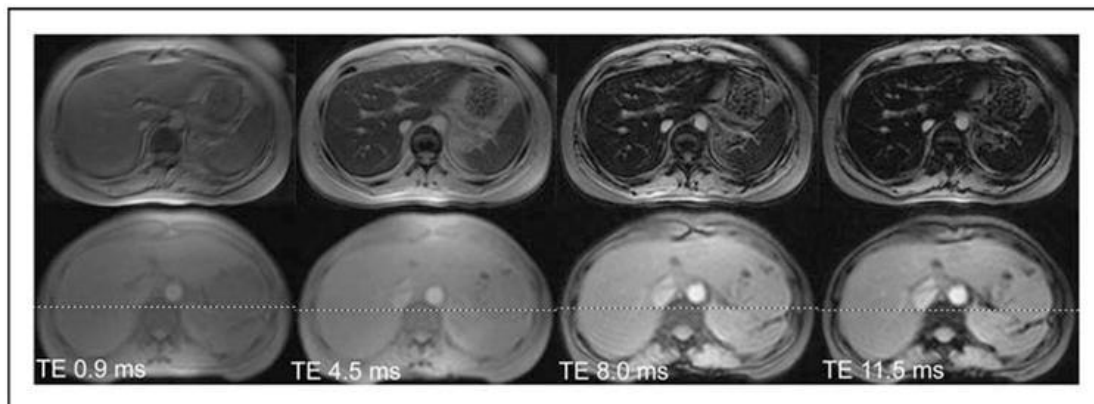
### **Validation of hepatic iron measurements**

Liver disease is a common complication in older thalassemia patients. Common causes of liver disease include iron overload, transfusion-related viral hepatitis (Hepatitis B, C), drug toxicity and biliary disease due to gallstones (6).

The liver accounts for approximately 70%–80% of the total body iron stores in iron overloaded patients. As a result, changes in liver iron accurately predict the balance between transfusional burden and iron removal therapies. LIC exceeding 17 mg/g dry weight are associated with iron-mediated hepato-cellular damage. (6).

Patients with LIC values above this threshold are also at increased risk for cardiac iron overload. Long-term liver siderosis is associated with increased risk of hepatocellular carcinoma in patients with hereditary hemochromatosis. Hepatocellular carcinoma is also becoming a leading cause of death in iron-loaded adults with thalassemia syndromes, even in patients that are hepatitis C negative. (4)

Liver T2\* value: generated by a transverse slice through the liver was obtained during a single breath-hold multi-echo gradient echo sequence with 12 echo times ranging between approximately 1 and 15 ms, depending on the scanner. From these images a T2\* map of the imaged liver slice are generated, with T2\* measured manually from a given region of interest. (7)



### Gradient echo images of liver collected at four different echo times

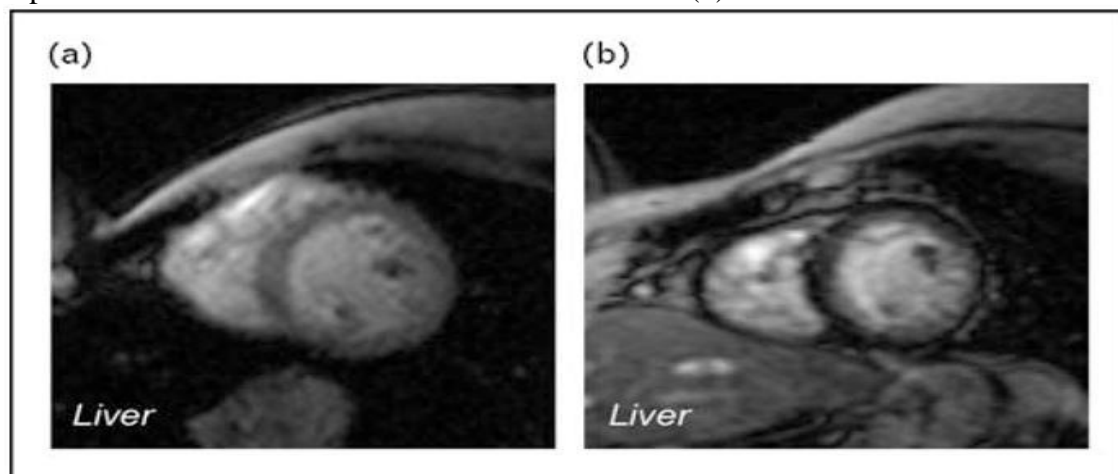
The top four images were collected from a patient having a liver iron of 6 mg/g. The bottom four images were collected from a normal volunteer. All images darken as the echo time (TE) lengthens, but the iron-heavy tissue darkens faster. The half life of this process is called T2\* and the rate is called R2\* ( $R2^* = 1000/T2^*$ ). (8)

### Interpretation of results of MRI T2\*

A liver T2\* value < 1,8 ms was considered indicative of a significant load. Using the calibration curve introduced by **Wood et al.**, (1) the cut-off corresponds to a liver iron concentration (LIC) is  $\geq 3$  mg/g/dw. Following the thresholds proposed by **Angelucci et al**, (9) severe liver iron overload was considered present with a LIC >15 mg/g/dw (T2\* value < 1.8 ms).

### Limitations of LIC: need to image other organs

Although LIC is a good surrogate for total body iron flux, the majority of iron toxicities occur in extra-hepatic tissues. These iron-sensitive “target” organs have different mechanisms and kinetics of iron uptake/clearance than the liver. In particular, endocrine tissue and the heart almost exclusively absorb NTBI species, whereas liver iron uptake is predominantly transferrin mediated. (10) As a result, iron chelation administered is unlikely to prevent cardiac and endocrine iron deposition. The different iron uptake kinetics between liver and heart causes ferritin and liver iron values to have little predictive value for cardiac iron deposition when evaluated on a cross-sectional basis. (1)



### Gradient echo (T2\*) imaging illustrating discordant iron loading of the liver and the heart

(a) Heavy liver iron loading (dark tissue) with heart sparing. (b) Heavy cardiac iron loading with no liver iron deposition. (1)

High LICs can place patients at cardiac risk indirectly by increasing circulating NTBI species. In these patients, missed chelator doses leave extrahepatic organs exposed to high NTBI. However, some patients have fully saturated transferrin and high NTBI levels even if their LIC is well controlled, leaving them at risk for endocrine and cardiac iron accumulation. (11).

The ability of MRI to document preclinical extra-hepatic iron deposition has transformed our ability to manage patients safely and has provided insights into the kinetics of iron loading/unloading in different organs and chelator access to these different tissue iron pools.

(11).

### Validation of cardiac iron measurements

Cardiac complications are the usual causes of heart failure in patients with B-thalassemia. Although anemia itself can be a cause of cardiac signs, the iron overload causes the severe and usually permanent damage. The so called "iron induced" cardiac complications include recurrent pericarditis, various form of heart block, ventricular ectopic beats, ventricular tachycardia, cardiomegaly with deteriorating left ventricular function and ultimately refractory congestive heart failure are the leading cause of death in beta thalassemia patients (12).

**Carpenter et al** reported a worldwide survey of cardiac MR  $T_2^*$  that shows a moderate or severe cardiac iron overload condition at initial cardiac MR scanning. [1](#) To avoid this condition, early detection of iron loading by  $T_2^*$  measurement is needed and followed by an appropriate iron chelation therapy to improve the survival rate of hemochromatosis. Several studies reported a reduction of age recommendation to start the first  $T_2^*$  screening for thalassemia major patients at 5 years old.

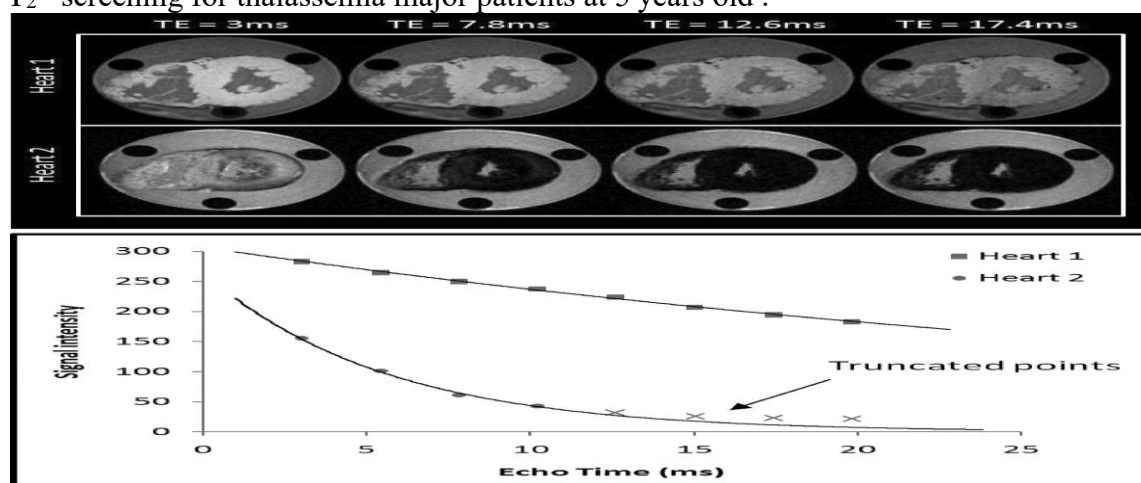


**Figure 2.** Example of cardiac  $T_2^*$  scans. Representative images of 2 hearts are shown at increasing echo times (TE) from 3 to 17.4 milliseconds. Heart 1 has normal iron levels and remains bright, whereas heart 2 (which has severe iron loading) shows progressive darkening with increasing echo time. The graph shows signal intensity (arbitrary units) plotted against echo time (milliseconds) for the hearts shown on top. Heart 1 has a shallow decay curve with  $T_2^*$  value of  $>20$  milliseconds. Heart 2 has a much more rapid decay with  $T_2^* < 10$  milliseconds. (13)

The  $T_2^*$  imaging in myocardial iron overload measurement: using a bright-blood or black-blood gradient echo sequence, Image series should be acquired at eight TEs ranging from 1–18 msec. some delay : 10 msec after the R-wave at the end-diastolic phase to obtain images avoiding heart motion artifact. (7)

When applying the bright-blood MGE at 1.5T MRI, the limited contrast between the myocardium and its surroundings is a major concern inferring with accurate delineation of endocardial and epicardial borders, artifacts tend to appear at different TE images of the myocardium which may lead to overestimation of the amount of iron deposited in the myocardium. (7)

Another method to generate a series of MGE images is known as the black-blood sequence. Here the blood pool signal is suppressed by double inversion pulses improving the contrast between myocardium and its surroundings and to remove any blood signals inducing susceptibility artifact. (7)

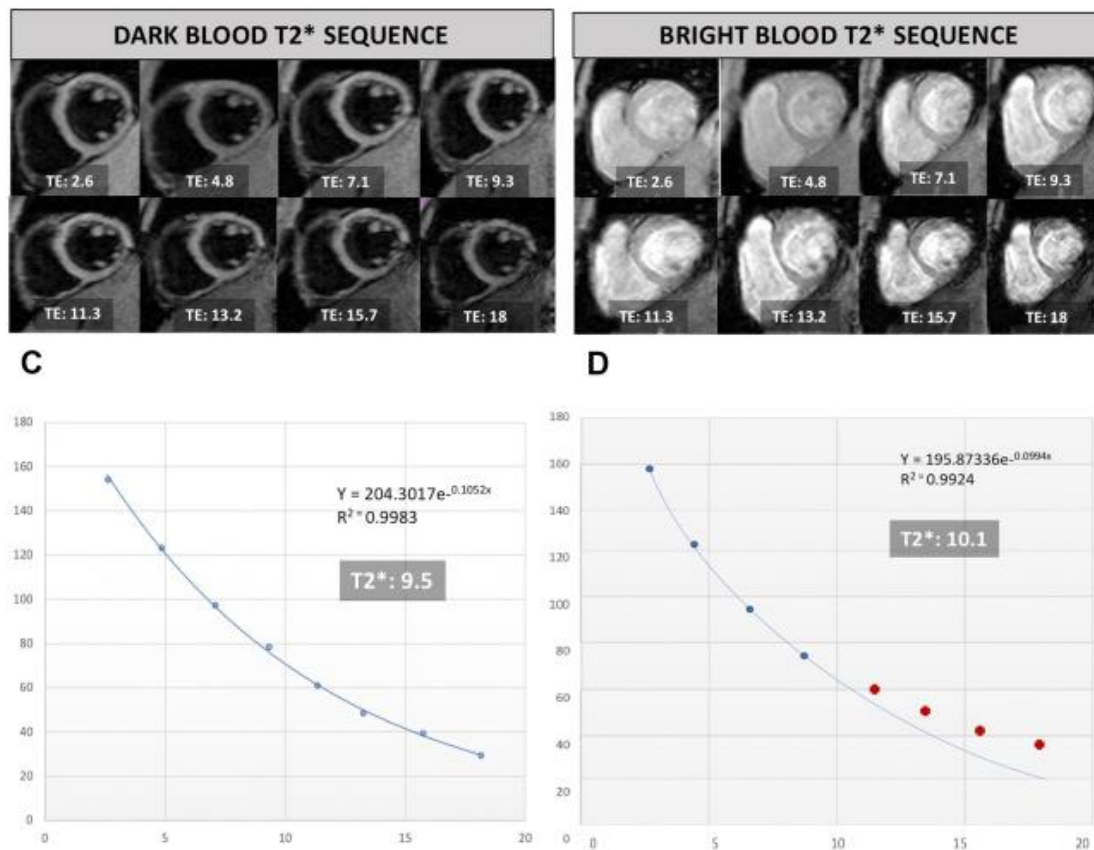


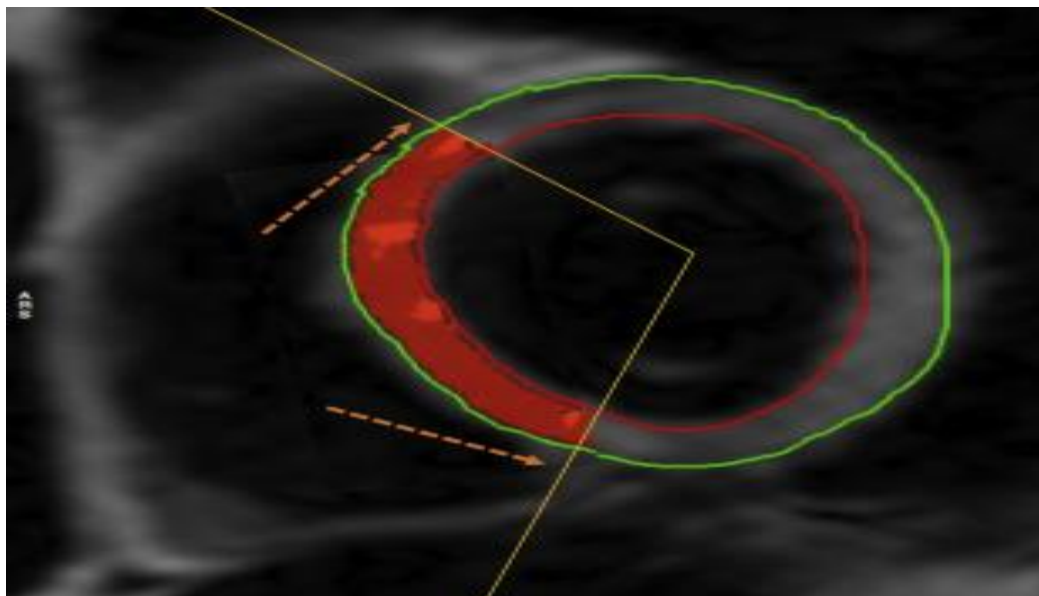
Fig.

(A, B) Midventricular short-axis image at different TE between 2 and 18 milliseconds in a patient with  $\beta$ -thalassemia. Image quality of black-blood sequence is superior (less artifact susceptibility) compared with bright-blood image. (C) Dark-blood image analysis. Background noise is reduced and curve shows a good fit for the 8 GRE time without the use of truncation ( $R^2 = 0.9983$ ,  $T2^* = 9.5$  milliseconds). This technique reduces the risk of errors during analysis. (D) Bright-blood image analysis. The last 4 points (red circle) are below the background noise and are removed to improve the curve fit using the truncation method ( $R^2 = 0.9924$ ,  $T2^* = 10.1$  milliseconds). (14)

### Post-processing and Myocardial T2\* Calculation

The measurement of myocardium iron is typically performed in a mid-ventricular short-axis image. The septal iron concentration largely reflects the global iron content as shown in biopsy studies, so analysis can be restricted to this segment to avoid artifacts caused by susceptibility effects (15).

The  $T_2^*$  value is derived by fitting signal intensities of mid-septal region of interest (ROI) including both epicardial and endocardial contours drawn on a short-axis image and propagated to all TEs



Midventricular short-axis slice of the heart showing the correct assessment of iron quantification with T2\* method. Full-thickness region of interest is defined by limiting the epicardial and endocardial border (gradient infiltration starting at epicardium). Analysis is restricted to the septum ( *yellow lines* ), in order to avoid artifacts from anterior and posterior cardiac veins ( *orange arrows* ) and the lung.( **15**)

#### Interpretation of results of MRI T2\*

The T<sub>2</sub>\* value detects iron overload status in blood disease patients. On its detection, Cardiac T<sub>2</sub>\* >20 msec reflects no cardiac iron overload Values of 20ms as low, between 20-10 ms as intermediate and < 10 ms as high risk (**16**).

Heterogeneous iron distribution in the myocardium has been demonstrated in histological studies, and this would suggest the necessity for global MRI estimation of myocardial iron (**15**). using T<sub>2</sub>\* multiecho cardiac MRI, demonstrated that global T<sub>2</sub>\* shows a close correlation with midseptal T<sub>2</sub>\*, suggesting that the latter may be used for a quick assessment of myocardial siderosis.

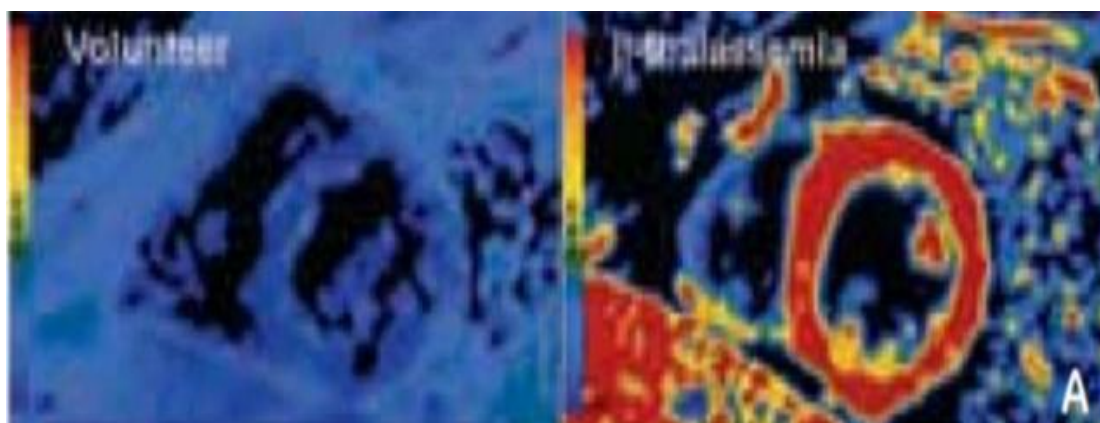


**Figure (20):** T<sub>2</sub>\* iron content color maps of the heart in a normal volunteer and in patient with  $\beta$  thalassemia (**15**). The diagram shows Scale of the color image: Blue = low iron content; Red = high iron content. A. Short axis T<sub>2</sub>\* color map of the heart in a normal volunteer shows low iron content (left ventricle shows blue coloring). Short axis T<sub>2</sub>\* color map in a patient with  $\beta$  thalassemia shows high iron content (left ventricle shows red coloring).

Heart take up circulating labile iron species that are not bound to transferrin (so-called NTBI), while liver iron uptake is predominantly mediated via transferrin. As a result, serum ferritin and liver iron values have almost no predictive value for cardiac iron deposition when evaluated on a cross-sectional basis (5)

Differences in iron kinetics and more active elimination of iron from the hepatocytes than from the myocytes may be responsible for the lack of correlation of the MRI-determined myocardial iron with that of the liver in patients receiving chelation therapy.(17)

MRI has also been used to characterize tissue iron deposits in the brain, pituitary gland, bone marrow, kidney and pancreas , Although less well validated and clinically exploited, these approaches are likely to become increasingly important in the assessment of transfusional iron overload (18)

### Pancreas Iron

#### Impaired glucose tolerance and diabetes mellitus:

are frequently observed complications in patients with thalassemia , may be the consequence of beta cell destruction secondary to chronic liver disease, iron overload ,viral infection and genetic factors and more effective iron chelating appears to improve glucose intolerance (19).

The pathogenesis resembles type-2 diabetes Iron deposition in the liver may produce insulin resistance by interfering with the ability of insulin to suppress hepatic glucose production. It was found that the incidence of diabetes mellitus was lower in those receiving good chelation. Diabetes in thalassemia is rarely complicated by ketoacidosis (19).Diabetes mellitus increases the risk for cardiac complications, heart failure, hyperkinetic arrhythmias and myocardial fibrosis irrespective of myocardial iron overload (15).

MRI quantitatively assess pancreatic iron loading in transfusion-dependent thalassemic patients.. pancreas R2\* values offer complementary information to liver and heart iron estimates. Because the pancreas takes up similar iron species as the heart, but earlier, it serves as an early and robust marker of prospective cardiac risk. A “clean” pancreas has nearly 100% negative predictive value for cardiac iron deposition. (18)

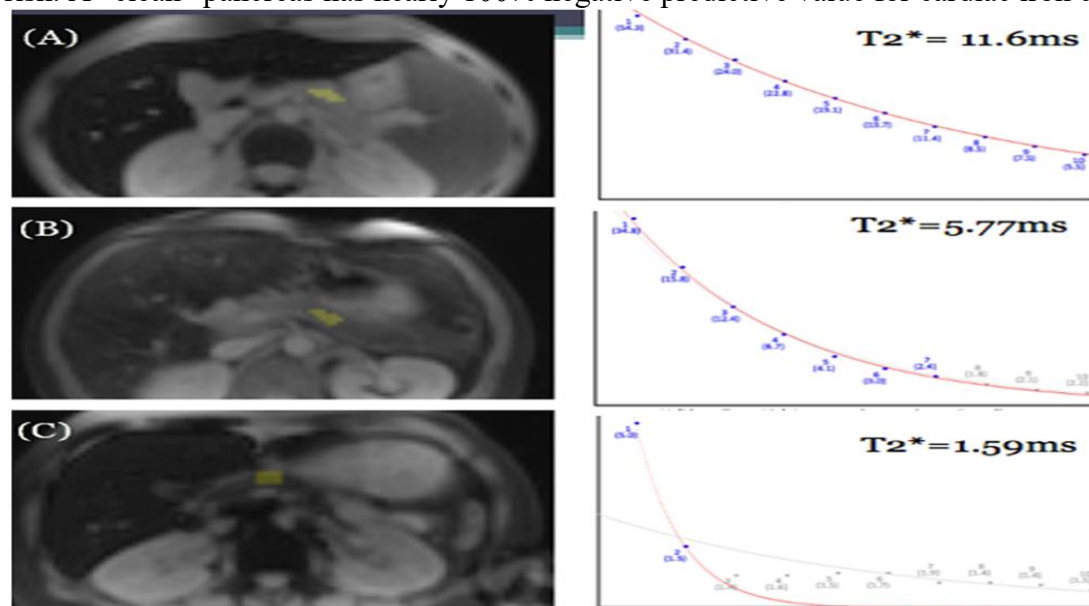


FIGURE 1. GRE MRI images of three different patients showing mild (A), moderate (B), and severe (C) iron deposition in the pancreas at the level of the splenic vein, and corresponding differences in rate of signal decay resulting in different pancreatic T2\* values in patients with mild, moderate, and severe pancreatic iron overload. (18)

### Pituitary Iron

#### Growth retardation, short stature, Delayed Puberty and Hypogonadism:

is one of the commonst typical findings in thalassemia major patient under transfusion not properly chelated thalassemic patients. thought to be a result of iron overload which leads to damage at pituitary, hypothalamic

or gonadal level. Other contributing factors include chronic anemia, transfusional iron overload, hypersplenism and chelation toxicity (19)

Early detection of pituitary iron overload is important since hypogonadism is not fully reversible by iron chelation. MRI has been used to predict asymptomatic iron deposition in the heart, liver, pancreas, and pituitary gland (20)

Patients with transfusion iron overload begin to develop pituitary iron deposition since during the first decade of life but clinical manifestations are usually not evident until the onset of puberty. (21)

At the earlier stage, only a diminished gonadotropin reserve with intact gonadotropin pulse was observed. until the second to third decade of life, significant pituitary volume loss especially a Z-score of pituitary volume lower than  $-2.5$  or pituitary height less than 4.4 mm due to apoptosis of gonadotropic cells, the gonadotropin reserve significantly diminishes, with markedly reduced spontaneous pulsatile gonadotropin activity which may lead to irreversible damage of the HPG axis. (18)

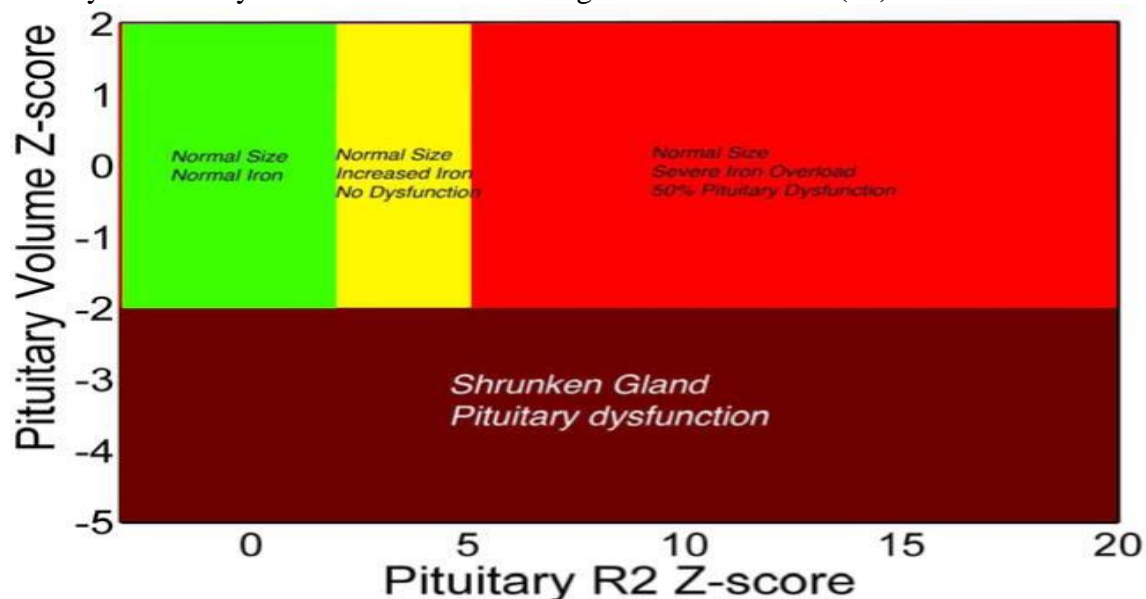
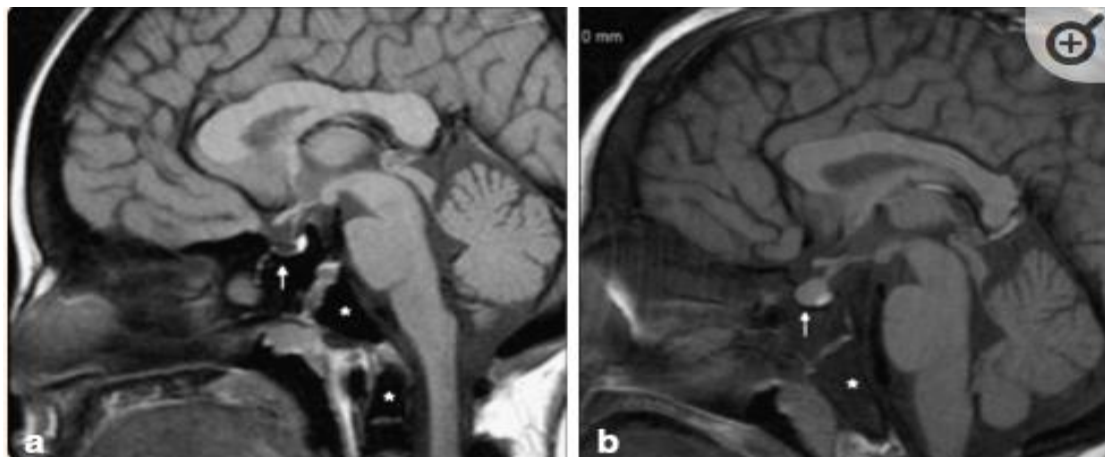


[Figure 6](#)

Plot of pituitary size (Z-score) versus pituitary iron. No pituitary dysfunction was observed when size and iron Z-scores were normal (green) or even when pituitary iron was moderately elevated (Z score 2 to 5, yellow zone) However, hypogonadism was common (50%) in severe pituitary iron overload ( $Z > 5$ , red zone) or when the pituitary gland was shrunken (Z score  $< -2.0$ ).

However, MRI results reveal that many patients with moderate to severe pituitary iron overload retain normal gland volume, representing an opportunity for iron chelation treatment and potential improvement in pituitary function. (18)





The pituitary. **a** A 12-year-old male with  $\beta$ -thalassaemia major. Midsagittal T1-weighted (TR/TE 500/20 ms) scan shows low-signal intensity of the anterior pituitary lobe (*arrow*) and the bone marrow (*asterisks*) suggesting iron overload. The pituitary gland is small measuring 3.5 mm (normal for age  $5.3 \pm 0.8$  mm). This patient developed hypogonadotropic hypogonadism. **b** An 11-year-old male with  $\beta$ -thalassaemia major. Midsagittal T1-weighted (TR/TE 500/20 ms) scan shows normal signal intensity of the anterior pituitary lobe (*arrow*) along with normal pituitary gland height (6 mm). The bone marrow (*asterisk*) shows low-signal intensity suggesting iron overload (22)

Iron deposition in the anterior pituitary gland can decrease pituitary MRI signal intensity significantly in the T2-weighted image. MRI signal hypointensity is due to the paramagnetic effect of iron, and serves as a useful tool for early detection of pituitary iron overload. (21)

anterior pituitary gland height was measured as the distance between the superior and inferior borders of the gland on the midline sagittal images Pituitary-R2\* measurement of a  $\beta$ -TM patient using an analytic software. (a) In a single coronal plane, image centered on the anterior pituitary gland was chosen at first echo time. (b) A full-thickness ROI was drawn to cover the visualized anterior pituitary lobe of the first echo. (c) Signal intensity decay of this region for each echo time was calculated with relaxometry technique by the software (22)

Although liver iron concentration has been considered to be an excellent marker of total body iron load, no relationship has been found between liver and pituitary iron deposit using MRI, No association between MRI parameters of siderosis in the pituitary gland and in other solid organs has been demonstrated, The lack of correlation may be due to differences in transferrin receptor concentration, iron kinetics, and the degree of organ inflammation or fibrosis.(2)

A lack of correlation between R2 and serum ferritin was found, possibly because serum ferritin, which does not cross the blood–brain barrier, is not a good marker of brain siderosis. (2)

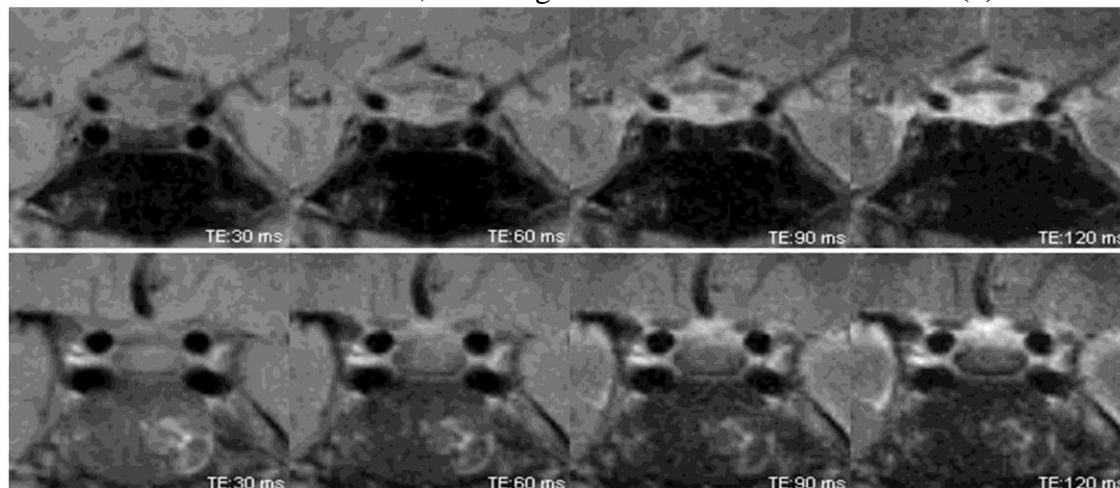


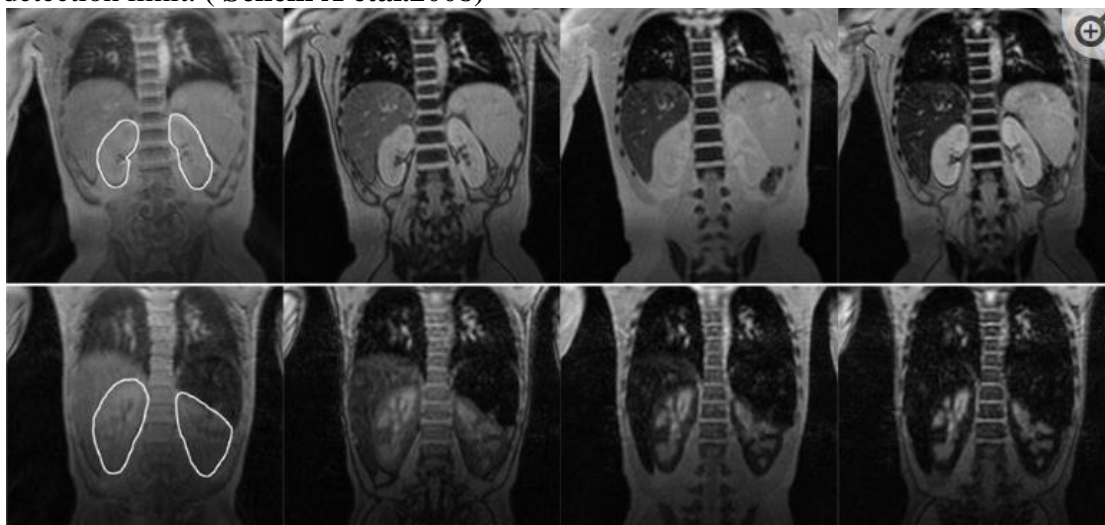
**Fig. 6.** Coronal T2-weighted spin-echo images of anterior pituitary gland at four different echo times (TE = 30, 60, 90, 120 ms). (a) Images from a 29-year-old  $\beta$ -TM patient with HH (top row). (b) Images from a 26-year-old  $\beta$ -TM patient without HH (bottom row). As the TE gets longer, the resultant images become hyposignal; however, the tissues with iron accumulation do so more rapidly. (22)

### **Kidney**

Evidence of proximal tubular damage is observed in patients with beta thalassemia major, derived from the destruction of membrane lipids by peroxidation **due to** Iron overload, too aggressive iron removal and the underlying anemia (22).

Decellularized hemoglobin (also known as plasma free hemoglobin) is filtered at the glomerulus and NTBI uptake and storage throughout the different renal cell-types creates a characteristic cortical darkening on a multiecho-gradient echo T2\* MRI images, with complete sparing of the medulla (23)

No correlations have been observed between kidney R2\* and liver iron concentration in patients with thalassemia. While we cannot exclude that iron plays a role in the pathophysiology of this tubular dysfunction, our data suggests that renal iron toxicity in thalassemia would have to occur at concentrations below the MRI detection limit. (Schein A et al.2008)



### **Comparison of kidney T2\*-weighted images in two thalassemic patients**

Representative T2\*-weighted coronal MR images of the kidneys at the first four echo times (TE) from a 10-year-old with thalassemia (top) demonstrates little kidney darkening or tissue contrast with increasing echo time with mean kidney R2\* value of 17 Hz and a 14-year-old with thalassemic (bottom) exhibits striking cortical darkening with mean kidney R2\* values of 180 Hz. The region of interest for analysis is shown in the leftmost images. (23)

### **Bone marrow**

Despite blood transfusion controlling bone marrow expansion and maintaining acceptable Hb levels, chelation treatment preventing bone iron toxicity and adequate sex hormone replacement correcting hypogonadism, a wide spectrum of bone abnormalities still affect thalassemic patients. The entity defined as “thalassemic osteopathy” includes osteopenia/ osteoporosis, fractures and spinal complications. Osteopenia or osteoporosis is seen in approximately half of the even well-treated thalassemia major patients. The delay in sexual maturation, the presence of diabetes and hypothyroidism, the parathyroid gland dysfunction, the progressive marrow expansion, the iron toxicity on osteoblasts, the iron chelators and the deficiency of growth hormone (GH) or insulin growth factors (IGFs) have been identified as major causes of bone loss in thalassemia major (24).

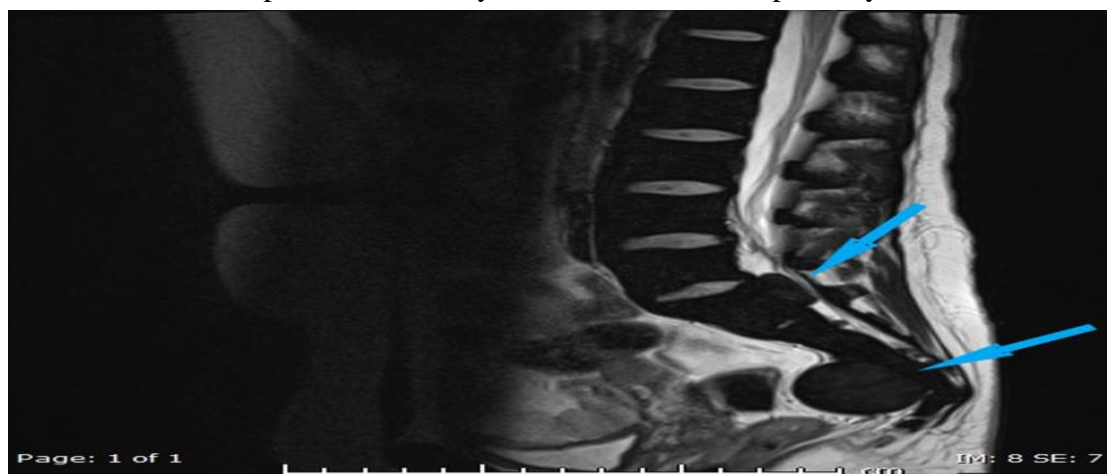
Bone marrow T2\* measurements can be easily obtained using the same sequences acquired for liver iron quantification. An axial slice in the upper abdomen was acquired by a T2\* gradient-echo multiecho sequence and the T2\* value was calculated in a circular region of interest defined in the visible body of the first or second lumbar vertebra. A positive correlation was found between bone marrow and heart T2\* values ( $R = 0.143$ ;  $P = 0.018$ ). A normal bone marrow T2\* showed a negative predictive value of 100% for cardiac iron. (25)

Sagittal T2 WI of the LSS shows diffuse low-signal intensity of the bone marrow of LSS (known case of thalassemia major) with well-defined mass of the same signal intensity ( $5.3 \times 3$  cm) in presacral region (blue arrow) and another similar smaller mass ( $2 \times 1$  cm) in anterior extradural space posterior to S1 level (Blue arrow) extramedullary haematopoiesis with cortical bone thinning. The thickened trabeculae appear as hypointense bands within the expanded marrow space

(26).

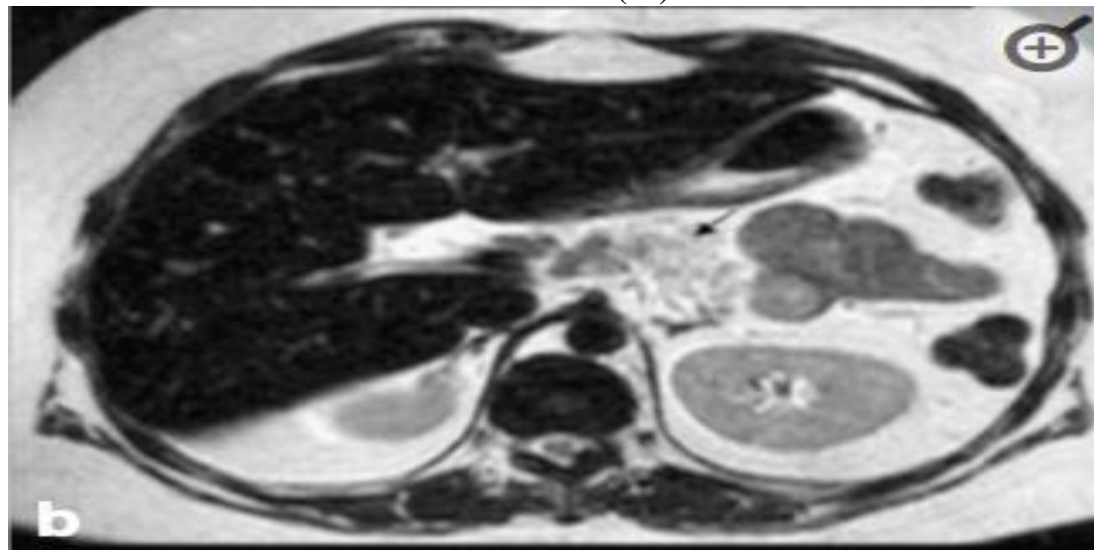
### Adrenal Iron

In iron overloaded patients a variety of abnormalities of pituitary adrenal axis have been reported with



adrenocorticotrophic hormone (ACTH) deficiency and reduced adrenal cortical reserve secondary to iron deposition in zona glomerulosa (site of mineralocorticoid production). Clinical adrenal deficiency is a very rare complication in well chelated thalassemia patients. (27).

There is only one study evaluating adrenals for iron overload with MRI, which showed a significant correlation between adrenal and liver siderosis (27).



A 27-year-old-male with  $\beta$ -thalassaemia major and diabetes. Axial T2-W (TR/TE 1,800/80 ms) scan shows low-signal intensity of the liver and adrenals suggesting siderosis. (28)

### Spleen iron

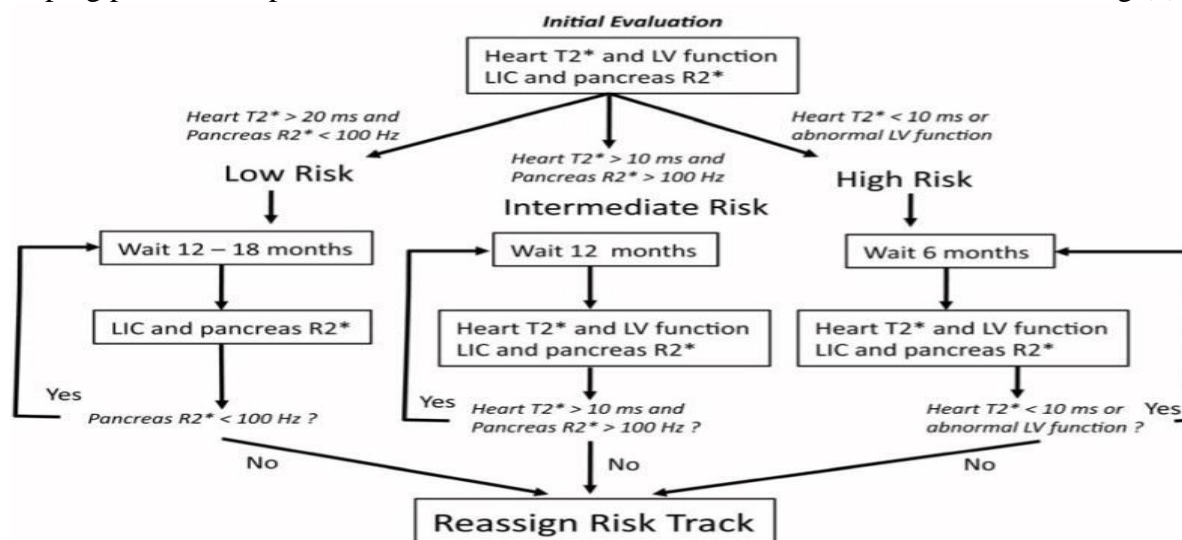
Enlargement of the spleen occurs as a result of excessive red cell destruction, extramedullary hemopoiesis and later because of iron overload. In an effort to cope with the increased demands made on it, the spleen often becomes hyperactive - a condition known as hypersplenism - and in this process also destroys the normal red blood cells the patient receives from blood transfusions. As a result, the patient requires more blood at each transfusion, but the transfusions fail to have an effect on the anemia. A hyperactive spleen may also destroy other components of the blood, such as white blood cells and thrombocytes (29).

Spleen  $R2^*$  values are easy to measure using the same analysis and acquisition techniques as the liver. No  $R2^*$  – iron calibration curve has been directly validated, but indirect methods have been applied. No functional significance for spleen iron accumulation has been determined to date. (30)

### Rational monitoring practices

MRI  $T2^*$  evaluation is often performed yearly for surveillance of organ iron load, but can be performed more frequently if needed. Indications for MRI surveillance for heart and liver iron load are based upon individual patient transfusion, iron chelation history and laboratory evaluation including serum ferritin values.  $T2^*$  imaging can be performed even in very young children, but may not be clinically necessary until later in childhood or adolescence with routine imaging surveillance continuing into adulthood (1)

Patients are generally followed by hematologists and/or cardiologists for changes in heart or liver  $T2^*$  values that may lead to a need for a change in chelation therapy with the goal of reducing organ iron overload and helping prevent complications such as iron overload related heart failure from occurring (9).



Flow chart outlining our recommended monitoring algorithm.

Low risk patients only need MRI examination of the abdomen, because a “clean” pancreas guarantees that the heart is free from significant iron deposition. We define a “intermediate” risk patient as chronically transfused and having sufficient transfusional exposure (usually greater 7 years for a thalassemia major patient) to be at risk for cardiac iron overload. However, most patients receive heart and abdominal MRI examinations on the first visit because we are unsure of their complete transfusion and chelation history and because there can be genetic co-modifiers of cardiac risk. (1)

High risk patients are defined as those whose cardiac  $T2^*$  is less than 10 ms. We scan these patients at six month intervals for three reasons. Firstly, it is important to monitor their left ventricular function. We treat even minor decreases in ventricular function quite aggressively. Secondly, liver iron can change quite quickly during intensified therapy and it is important to avoid overchelation. Lastly, it provides important feedback to the patients who often struggle drug compliance. (1)

MRI is increasingly being used worldwide to follow organ iron overload in  $\beta$  thalassemia patients, but can also be used to assess other types of patients with iron overload states including sickle cell disease and hemochromatosis.

### References

1. Wood JC, Tyszka JM, Carson S, et al. (2004): Myocardial iron loading in transfusion-dependent thalassemia and sickle cell disease. *Blood* ; 103(5): 1934-1936.
2. Wahidiyat PA, Liauw F, Sekarsari D, et al. (2017): Evaluation of cardiac and hepatic iron overload in thalassemia major patients with T2\* magnetic resonance imaging. *Hematology*; 22(8): 501-507.
3. Argyropoulou, M., D. Kiortsis and L. Astrakas, (2007): Liver, bone marrow, pancreas and pituitary gland iron overload in young and adult thalassemic patients: a T2 relaxometry study. *Eur Radiol*, 17, 3025–3030.
4. Papakonstantinou, O. G., T. G. Maris and V. Kostaridou, (1995): Assessment of liver iron overload by T2-quantitative magnetic resonance imaging: correlation of T2-QMRI measurements with serum ferritin concentration and histologic grading of siderosis. *Magn Reson Imaging*, 13, 967–977.
5. Alexopoulou, E., F. Stripeli and P. Baras, (2006): R2 relaxometry with MRI for the quantification of tissue iron overload in betathalassemic patients. *J Magn Reson Imaging*, 23, 163–170.
6. Brissot P, Cappellini MD (2014): LIVER DISEASE. In: Cappellini MD, Cohen A, Porter J, et al., (Eds.). *Guidelines for the Management of Transfusion Dependent Thalassaemia (TDT)*. 3rd ed., Thalassaemia International Federation, Nicosia (CY). Chapter 5. PP. 143-159.
7. Shehata, S.M., Amin, M.I. & Zidan, E.S.H. MRI evaluation of hepatic and cardiac iron burden in pediatric thalassemia major patients: spectrum of findings by T2\*. *Egypt J Radiol Nucl Med* 50, 68 (2019).
8. Anderson LJ, Holden S, Davis B, et al. (2001): cardiovascular T2\* (t2star) magnetic resonance or the early diagnosis of myocardial iron. *Eur heart j*; 22(23): 2171-2179.
9. Angelucci E, Barosi G, Camaschella C, et al. (2008): Italian society of hematology practice guidelines for the management of iron overload in thalassemia major and related disorders. *Haematologica*; 93(5): 741-752.
10. Aessopos A, Farmakis D, Deftereos S, et al. (2005): Thalassemia heart disease: a comparative evaluation of thalassemia major and thalassemia intermedia. *Chest* ; 127(5): 1523-1530. Melbourne. PP. 321-331.
11. Dusheiko GM (2011): Overview of Hepatitis Associated Liver Disease in Thalassemia and Its Current Management. *Thalassemia Reports*; 2039 (4357): 11.
12. Tubman VN, Fung EB, Vogiatzi M, et al. (2015): Guidelines for the Standard Monitoring of Patients with Thalassemia: Report of the Thalassemia Longitudinal Cohort. *J Pediatr Hematol Oncol.*; 37(3): e162-169.
13. Christoforidis, A., A. Haritandi, I. Tsitouridis, I. Tsatra, H. Tsantali, S. Karyda, A. S. Dimitriadis and M. Athanassiou-Metaxa, (2006): Correlative study of iron accumulation in liver, myocardium, and pituitary assessed with MRI in young thalassemic patients. *Journal of pediatric hematology/oncology*, 28, (5) 311-315.
14. Xu F, Luo C, Li M, et al. Quantification of cardiac iron in patients with thalassemia with 3-T MRI calibrated by 1.5-T MRI. *Acta Radiologica*. 2023;64(6):2096-2103.
15. Pepe A, Meloni A, Borsellino Z, et al. (2015): Myocardial fibrosis by late gadolinium enhancement cardiac magnetic resonance and hepatitis C virus infection in thalassemia major patients.
16. Tanner MA, He T, Westwood MA, et al. (2006): Multi-center validation of the transferability of the magnetic resonance T2\* technique for the quantification of tissue iron. *Haematologica* ; 91(10): 1388-1391.
17. Porter JB (2011): Pathophysiology of Iron Overload in Thalassemia Syndromes. *Thalassemia Reports*; 2039(4357): 8.
18. Noetzli LJ, Mittelman SD, Watanabe RM, et al. (2012): Pancreatic iron and glucose dysregulation in thalassemia major. *Am J Hematol*; 87(2): 155-160.d.
19. Toumba M, Sergis A, Kanaris C, et al. (2007): Endocrine complications in patients with thalassemia major. *Pediatr Endocrinol Rev*; 5(2): 642-648.
20. Borgna-Pignatti, C., S. Rugolotto, P. De Stefano, H. Zhao, M. D Cappellini, G. C. Del Vecchio, M. A. Romeo, G. L. Forni, M. R. Gamberini and R. Ghilardi, (2004): Survival and complications in patients with thalassemia major treated with

- transfusion and deferoxamine. *Haematologica*, 89, (10) 1187-1193.
21. Vogiatzi MG, Macklin EA, Trachtenberg FL, et al. Differences in the prevalence of growth, endocrine and vitamin D abnormalities among the various thalassaemia syndromes in North America. *Br J Haematol*. 2009;146:546–556.
  22. Nayak, A.M., Choudhari, A., Patkar, D.P. et al. Pituitary Volume and Iron Overload Evaluation by 3T MRI in Thalassemia. *Indian J Pediatr* 88, 656–662 (2021).
  23. Gburek J, Birn H, Verroust PJ, et al. Renal uptake of myoglobin is mediated by the endocytic receptors megalin and cubilin. *Am J Physiol Renal Physiol*. 2003;285:F451–458.
  24. Terpos E (2011): Overview of Bone Disease Research in Thalassemia –Current and Future. *Thalassemia Reports*; 2039(4357): 17.
  25. Meloni A, Pistoia L, Restaino G, Missere M, Positano V, Spasiano A, Casini T, Cossu A, Cuccia L, Massa A, Massei F, Cademartiri F. Quantitative T2\* MRI for bone marrow iron overload: normal reference values and assessment in thalassemia major patients. *Radiol Med*. 2022 Nov;127(11):1199-1208
  26. Hajimoradi, M., Haseli, S., Abadi, A. et al. Musculoskeletal imaging manifestations of beta-thalassemia. *Skeletal Radiol* 50, 1749–1762 (2021).
  27. Guzelbey T, Gurses B, Ozturk E, et al. (2016): Evaluation of Iron Deposition in the Adrenal Glands of  $\beta$  Thalassemia Major Patients Using 3-Tesla MRI. *Iran J Radiol*; 13(3): e36375.
  28. Drakonaki E, Papakonstantinou O, Maris T et al (2005) Adrenal glands in beta-thalassemia major: magnetic resonance (MR) imaging features and correlation with iron stores. *Eur Radiol* 15:2462–2468.
  29. Hoffbrand AV, Taher A and Cappellini MD (2012): How I treat transfusional iron overload. *Blood* Nov; 120(18): 3657-3669.
  30. Brewer CJ, Coates TD, Wood JC. Spleen R2 and R2\* in iron-overloaded patients with sickle cell disease and thalassemia major. *J Magn Reson Imaging*. 2009;29:357–364.